AKADÉMIAI KIADÓ

Optimisation preparation, physicochemical properties, and glucose transport regulation by polysaccharides from Liubao brick tea

H.Q. Wang[1]* , Y.Z. Sun[1], B.B. Li[1] and W.W. Zhang[2]

[1] Zhengzhou Shuqing Medical College, Gongming Road, 450064 Zhengzhou, China

[2] Henan Provincial People's Hospital, Weiwu Road, 463599 Zhengzhou, China

ORIGINAL RESEARCH PAPER

Check for updates

ABSTRACT

In this study, a water-soluble novel polysaccharide called TPS was successfully prepared and isolated from Liubao tea. The optimal extraction conditions resulted in a yield of 10.70% for the crude TPS. The purified TPS exhibited unique physicochemical properties and structural characteristics. It was identified as an acidic polysaccharide with trace binding proteins, with a →4)-α-D-Galp-(1→) residue. The purified TPS had a dense and uneven appearance, potential crystallisation characteristics, and structural stability. Importantly, it demonstrated the ability to inhibit glucose transport in Caco-2 cells by down-regulating the expression of sodium/glucose cotransporter 1 (SGLT1) and glucose transporter 2 (GLUT2), leading to a hypoglycemic effect. These findings highlight the potential of TPS from Liubao tea as a functional food or additive with hypoglycaemic properties.

KEYWORDS

* Corresponding author. E-mail: wanghuiqin1616@163.com

AK Journals

1. INTRODUCTION

Diabetes mellitus, a prevalent metabolic disorder characterised by elevated blood glucose levels, presents a global public health concern (Zhu et al., 2021a). Although conventional approaches to diabetes management include medication, diet, and lifestyle adjustments (Zhu et al., 2020c), there is a growing interest in investigating the therapeutic potential of bioactive compounds derived from plants to complement existing treatments (Jones et al., 2019).

Liubao tea (LBT), a fermented dark tea from Guangxi province, China, has gained recognition for its cultural significance and sensory qualities (Zhu et al., 2021a, 2021b). Recent studies have revealed the presence of bioactive components in LBT, including polyphenols, alkaloids, pigments, and polysaccharides (PS), which contribute to its potential health benefits (Zhu et al., 2021a, 2021b; Wu et al., 2021). Despite its unique properties, the health effects and active constituents of LBT have received limited exploration compared to other dark teas (Zhu et al., 2021b).

PS, as a prominent bioactive component in tea, has gained considerable attention for its potential therapeutic effects, particularly in the management of diabetes (Wang et al., 2022). Tea PS derived from LBT has shown diverse bioactivities and potential for developing functional foods and therapeutics targeting metabolic diseases (Qin et al., 2021; Qiu et al., 2022). Optimising the extraction process is crucial to maximise the yield, purity, and bioactivity of LBT-PS (Zhu et al., 2021c; Wang et al., 2022). Additionally, a comprehensive understanding of their chemical composition and structural characterisation is essential for establishing structure-activity relationships and identifying potential applications in diabetes management.

This study employed hot water extraction to optimise the extraction process of LBT-PS, and their physicochemical composition and structural properties were thoroughly analysed. Additionally, the hypoglycaemic activity of the PS was preliminarily evaluated and mechanistically analysed.

2. MATERIALS AND METHODS

2.1. Chemicals and reagents

Liubao brick tea (LBT) was provided by Guangxi Wuzhou ShengyuanTea Co., Ltd (Wuzhou, China). DMEM complete medium was purchased from HyClone Co. (Los Angeles, USA). CCK-8 determination kit was purchased by Solarbio Co. (Beijing, China). SGLT1 and GLUT2 polyclonal antibodies were purchased from Abcam Co. (CA, USA). All other chemicals and solvents were of analytical grade.

2.2. Polysaccharide preparation and purification

2.2.1. Optimal extraction and purification of TPS. The Liubao brick tea (LBT, 3a, aged for 8 years), also known as Qiulan brick tea, mainly underwent three main steps, including stacking fermentation, steaming compression, and aging storage. The aging storage phase further consisted of three stages, including semi-cellar aging in the early stage, dry warehouse aging in the middle stage, and plate warehouse aging in the later stage. The dried LBT was subjected to two

rounds (4 h/occasion) of pretreatment with 85% ethanol to remove small-molecule impurities. The resulting residue was extracted with deionised water, and the supernatant was concentrated, followed by overnight storage with ethanol. The resulting precipitate was collected, and the extraction parameters including temperature (60–100 °C), liquid-solid ratio (5:1–30:1), and ethanol concentration (20–90%) were varied. The obtained pellet was treated with 15% tri-chloroacetic acid to remove proteins, followed by dialysis (cutoff of 3,500 Da, 48 h) and lyophi-lisation to obtain crude tea PS (TPS). A response surface methodology (Design-Expert 8.0.6 Trial, State-Ease, MN, USA) based on a central composite design (CCD) was used to analyse the effects of extraction parameters on the yield of crude TPS (Table S1), with a total of 17 experiments conducted. The detailed factors and levels used in the experiments are listed in Supplementary Table S2. Supplementary Tables can be found on the server of the Publisher.

Polysaccharide purification was performed as described by Zhu et al. (2019). The eluted fraction by 0.2 M NaCl was collected and used for further analysis.

2.3. Physicochemical composition

2.3.1. Chemical composition. The phenol-sulphuric acid method (Zhu et al., 2021c) was uti-lised to determine the total sugar content, while the meta-hydroxyphenyl method was used to measure the uronic acid content (Zhu et al., 2021c). The recognised Bradford method was employed to quantify the protein content (Zhu et al., 2020c).

2.3.2. Monosaccharide composition. The monosaccharide composition was measured accord-ing to previous reports (Zhu et al., 2020c). Initially, 5 mg of the sample was hydrolysed in 2 M trifluoroacetic acid for 2 h at 121 °C, dried with nitrogen, and washed with methanol. The dried residue was then dissolved in deionised water, filtered through a microporous 0.22-μm filter, and analysed using an anion-exchange chromatography system from Thermo Fisher Scientific (LA, USA) and a CarboPac PA-20 anion-exchange column (150 × 3.0 mm). Additionally, fucose (Fuc), rhamnose (Rha), arabinose (Ara), galactose (Gal), glucose (Glc), xylose (Xyl), mannose (Man), fructose (Fru), ribose (Rib), galacturonic acid (GalA), glucuronic acid (GulA), mannur-onic acid (ManA), and guluronic acid (GlcA) were utilised as monosaccharide standards.

2.3.3. Molecular weight (MW). As previously reported (Zhu et al., 2019), dextran standards were used to establish a standard curve.

2.4. Spectral analysis

2.4.1. Fourier-transform infrared (FT-IR) spectroscopy. A systematic scan of the PBS sample, which was mixed with 100 mg of KBr powder, was conducted using an infrared spectrometer (PE-1730, manufactured in Massachusetts, USA). The scan encompassed a range of wave numbers from 4,000 cm^{-1} to 400 cm^{-1}.

2.4.2. Nuclear magnetic resonance (NMR) spectroscopy. To obtain the NMR spectra, 20 mg of polysaccharide samples were dissolved in D_2O and subjected to three rounds of lyophiliaation. The final product was reconstituted in 0.5 mL of D_2O. The Avance III HD spectrometer (Bruker in Billerica, MA, USA) was used to collect the ^1H and ^{13}C NMR spectra.

2.5. Structural properties

2.5.1. Scanning electron microscopy (SEM). The surface morphology of the sample was examined using a HITACHI SU8010 scanning electron microscope (manufactured by JEOL in Tokyo, Japan) at magnifications of $10,000 \times$ and $15,000 \times$. Prior to imaging, 2 mg of the sample was affixed to a metal block using conductive adhesive and gold was deposited on its surface.

2.5.2. X-ray diffraction (XRD). The X-ray diffraction was conducted by a D8 ADVANCE X-ray diffractometer (Bruker, Billerica, Massachusetts, USA) with the following settings: tube voltage of 35 kV, tube current of 100 mA, scattering angle ranging from 5 to 70°, and an angle step of 0.05°.

2.5.3. Thermogravimetry (TG). The thermal stability of TPS was evaluated using a Simultaneous Thermal Analyser (NETZSCH STA 449F3, Selb, Free State of Bavaria, Germany). A 10-mg sample was subjected to heating at a rate of 10 °C per min under nitrogen protection, and its thermal behaviour was recorded over a temperature range of 30–800 °C.

2.6. Hypoglycaemic evaluation

2.6.1. Cell culture. Caco-2 cells (Chinese Academy of Science, Shanghai, China) were seeded in DMEM complete medium and then incubated at 37 °C and 5% CO_2.

2.6.2. Cytotoxicity assay. Cytotoxicity assay was conducted according to a report by Zhu et al. (2021c) with a slight modification. Briefly, Caco-2 cells were seeded in 96-well plates at a density of 1×10^4 cells/well and incubated for 48 h. After removing the medium, the cells were treated with various concentrations of TPS (200, 400, 600, 800, 1,000, 1,200 µg mL^{-1}) for 24 h. The normal control (NC) group received no sample treatment. Following that, the medium was replaced with a 10% CCK-8-containing medium and incubated for 1 h. The absorbance at 450 nm was measured.

2.6.3. Glucose transport determination. Caco-2 cells were seeded at a density of 1×10^5 cells/well on 12-well Transwell® plates and cultured for 21 d to form a dense monolayer. The differentiation of the cell monolayer was evaluated by measuring the transmembrane resistance. Subsequently, 0.5 mL of DMEM complete medium containing 25 mM glucose was added to the apical compartment, and 1 mL of PBS was added to the basolateral compartment. The cell monolayers were incubated with the corresponding interventions for 2 h. The glucose content in the basolateral compartment was measured using a glucose assay kit. The positive control was acarbose (200 µg mL^{-1}), and the negative controls were phlorizin (1 mM) and phloretin (1 mM) as SGLT-1 and GLUT-2 inhibitors, respectively. The sample groups were treated with different concentrations of TPS (200, 400, and 600 µg mL^{-1}), and the model control (MC) group received no sample treatment.

2.6.4. RT-qPCR and western blotting. RT-qPCR and western blotting assays were performed according to a previous report (Zhu et al., 2021a). The sequences of all primers used for RT-qPCR are displayed in Table S3.

2.7. Statistical analysis

The statistical data, obtained from three independent experiments, are presented as mean ± SD. The differences among the groups were analysed using a one-way ANOVA test, and a P-value of less than 0.05 was considered statistically significant.

3. RESULTS AND DISCUSSION

3.1. Optimal extraction

The single-factor experiment (Fig. 1A–C) demonstrated that extraction temperature, liquid-solid ratio, and ethanol precipitation concentration significantly influenced the yield of crude TPS. It could be seen from Fig. 1 that the temperature of 85 °C, the liquid-solid ratio of 12.5, and the ethanol concentration of 65% were the optimum single factor parameters. Based on optimal conditions, a CCD regression model was established (Table S2). The TPS yield ranged from 7.89% to 10.75%, indicating the substantial impact of different factors and levels on the crude TPS yield. The relationship between the TPS yield (Y) and the experimental factors could be explained by the quadratic regression equation (Table S4). The analysis of variance showed effectiveness, good fit of the model, and high reliability. Individual factor analysis revealed the liquid-solid ratio (B) having the greatest impact. The response surface and contour plots showed that the interaction between the liquid-solid ratio and extraction temperature was the strongest. The binomial regression model predicted the optimal process conditions for crude TPS extraction as 83.73 °C, 13.48:1, and 71.78%, resulting in a yield of 10.79%. Experimental validation under the optimised conditions (84 °C, 14:1, and 72%) confirmed the reliability of the model, with a measured yield of 10.70 ± 0.03%.

3.2. Preliminary physicochemical composition

The purified TPS (referred to as TPS hereafter) resulted in an assayed yield of 2.06%. Chemical composition analysis (Table S5) showed that it contained 93.17% total sugars and 0.95% water-soluble proteins, indicating the presence of bound proteins even after impurity separation. The TPS had a uronic acid content of 29.98%, indicating it was an acidic polysaccharide. The monosaccharide composition analysis (Fig. 2A) showed that TPS contained Fuc, Rha, Ara, Gal, Glc, Xyl, Man, GalA, and GlcA, with a molar ratio of 1.21:16.80:21.78:27.47:10.03:3.70:12.78:3.57:2.65. The MW distribution analysis (Fig. 2B) showed that TPS consisted of two different distributions: 8.75×10^7 Da (3.81%) and 8.87×10^6 Da (96.19%). In comparison to TPS extracted from most green teas using hot water, the MW of TPS obtained from LBT was smaller, which could be attributed to the fermentation process during LBT production. Due to the non-fermented nature of green tea, the MW of TPS in Liubao tea is reduced through a process of deep fermentation (Qin et al., 2021).

3.3. Physiochemical and structural properties

The FT-IR spectrum of TPS (Fig. 2C) displayed several characteristic absorption peaks of PS bound to trace proteins, including 3,400–3,300 cm^{-1}, 2,921 cm^{-1}, 1740 cm^{-1}, 1,600 cm^{-1}, 1,400 cm^{-1}, and 1,050 cm^{-1} (Zhu et al., 2020a, 2020b, 2022). In the ^{1}H NMR spectrum of TPS (Fig. 3A), a signal peak with a chemical shift value of 5.06 suggested the presence of α-D-Galp-(1→H-1,
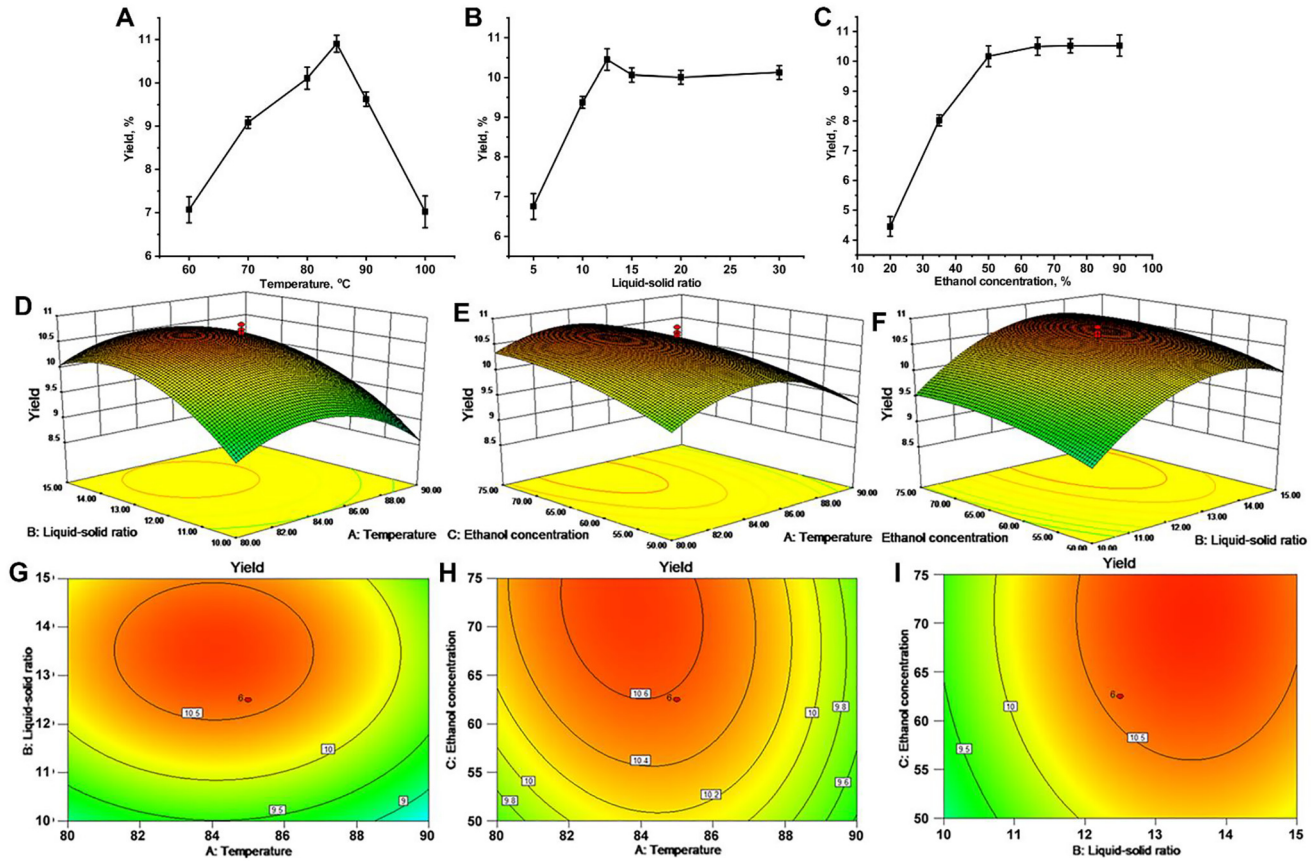
Fig. 1. Single-factor conditions, including the extraction temperature (A), liquid-solid ratio (B), and ethanol precipitation concentration (C). Response surface plots for (D, G) Y = f (B, A), (E, H) Y = f (C, A), and (F, I) Y = f (C, B)
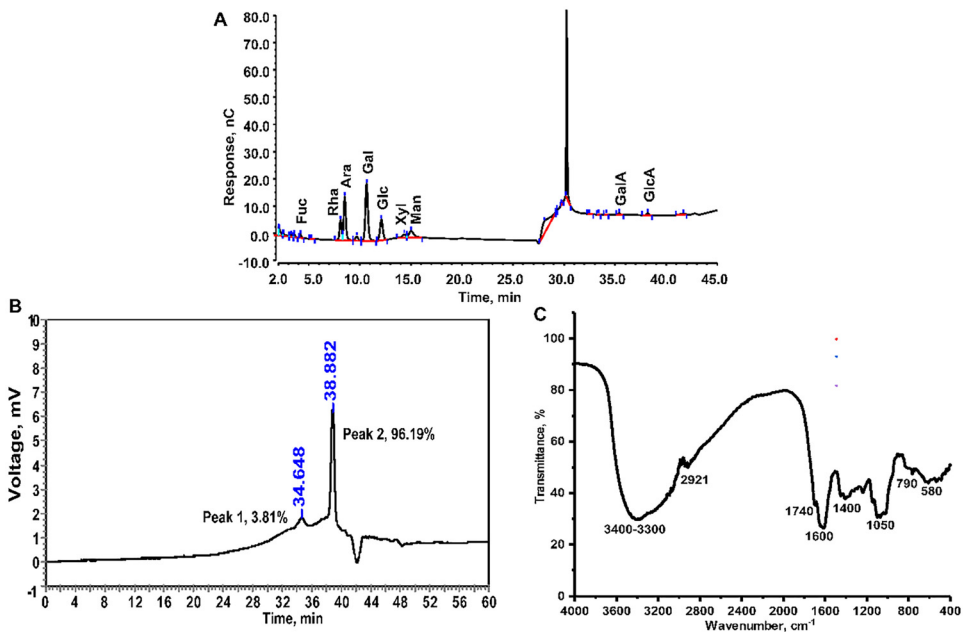
Fig. 2. Anion-exchange chromatography of monosaccharide compositions (A), HPGPC profile (B), and FT-IR (C) of TPS

which was further supported by the ^{13}C NMR spectrum (106.99 ppm) (Fig. 3B) (Shen et al., 2018). Additionally, the chemical shift between C2 and C5 indicated the presence of a (1→4)-bond (Li et al., 2019). Thus, it could be deduced that →4)-α-D-Galp-(1→ was one of the dominant monosaccharide residues in TPS.

The SEM image (Fig. 4A) showed a sheet-like surface of TPS that was relatively dense and bumpy. This uneven surface contributes to an increased specific surface area, which can enhance its bioactivity (Zhu et al., 2021c). XRD analysis (Fig. 4B) exhibited a significant diffraction peak at 22.5°, indicating the potential crystallisable property of TPS (Zhu et al., 2021c). TG analysis (Fig. 4C) demonstrated that TPS experienced two phases of weight loss, with a total weight loss of 59.62%, suggesting a favourable structural stability.

3.4. Hypoglycaemic evaluation

In vivo experiments have demonstrated the hypoglycaemic activity of LBT and its active ingredients (Zhu et al., 2021b). Figure 5A showed that the cell viability of Caco-2 cells was approximately 80% at concentrations of 1,000 and 1,200 µg mL^{-1} of TPS. Based on this, concentrations of 200, 400, and 600 µg mL^{-1} of TPS were selected for subsequent experiments. By measuring the amount of glucose transported from Caco-2 cells over a 2-h period, TPS at concentrations of 200, 400, and 600 µg mL^{-1} resulted in inhibition rates of 41.89%, 57.69%, and 68.19%, respectively (Fig. 5B). Acarbose exhibited a higher inhibition rate of 91.17%. Phlorizin had an inhibition rate of 60.81%, similar to TPS at 400 µg mL^{-1} but lower than

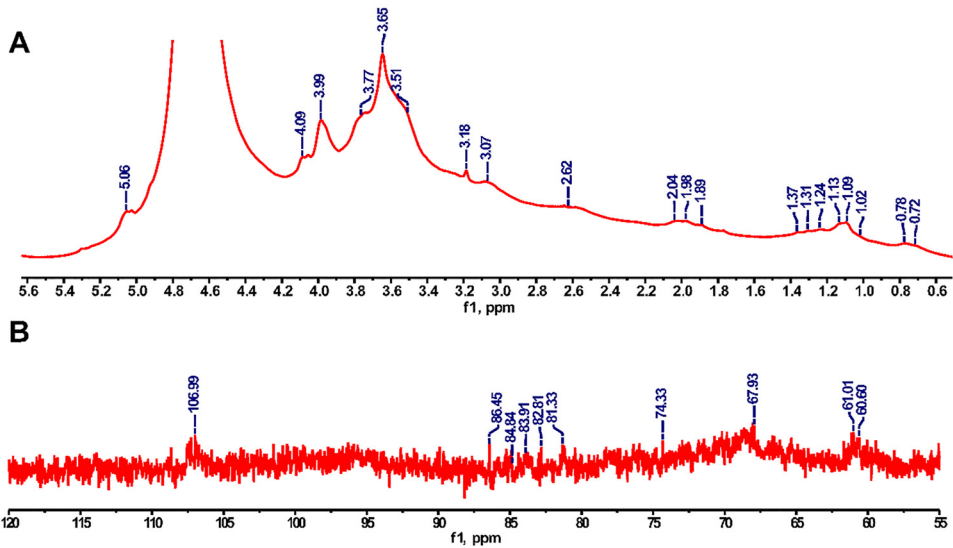*Fig. 3.* ^{1}H NMR (A) and ^{13}C NMR (B) spectra of TPS

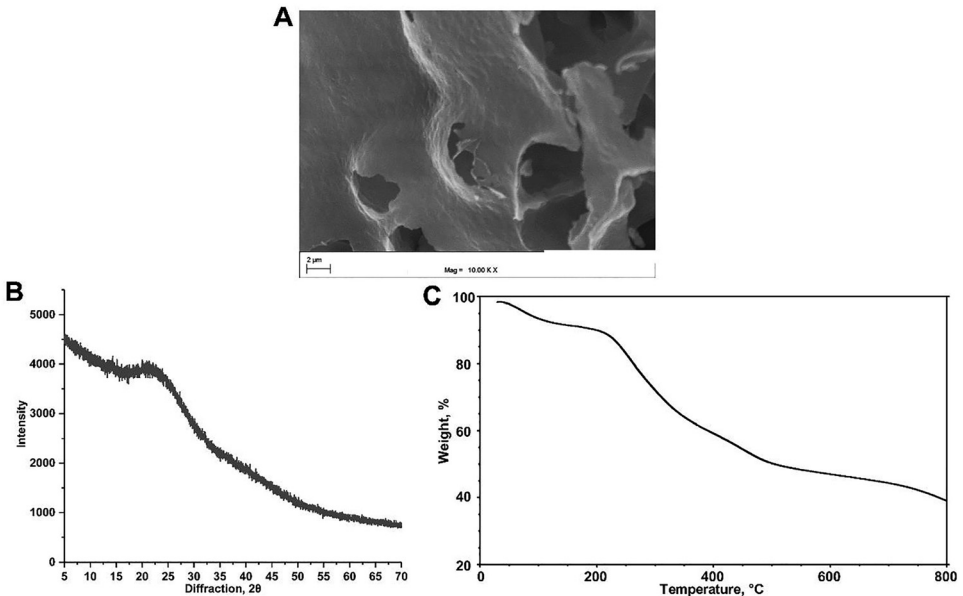*Fig. 4.* SEM (A), XRD (B), TG (C) of TPS

600 µg mL^{-1}. Phloretin showed the lowest inhibition rate of 20.79%. These results suggested that the inhibition of SGLT1 was involved in glucose transport inhibition, and TPS might act similarly to phlorizin. Previous studies had reported that Liubao tea had excellent

hypoglycaemic effects and alleviated insulin resistance, with TPS identified as a major contributor (Zhu et al., 2021a), which was supported by our findings. The significant inhibition rate of TPS might be attributed to its unique chemical composition and structural properties. TPS contained a substantial amount of uronic acid, which contributed a unique five-membered or six-membered carbon ring to regulate the activity of glucose metabolism enzymes and exerted a hypoglycaemic effect (Zhu et al., 2021c). Additionally, the high proportion of Gal in TPS was known to be closely related to the hypoglycaemic activity of tea polysaccharides (Zhu et al., 2021c). Meanwhile, the lower MW of TPS further contributed to its hypoglycaemic activity (Zhu et al., 2021c; Wang et al., 2022).

Studies have shown that SGLT1 plays a crucial role in glucose uptake and is a target for regulating hyperglycaemia with tea extracts (Liu et al., 2021). Knockout mice lacking SGLT1 have been shown to exhibit impaired glucose and galactose absorption (Kellett and Brot-Laroche 2005). Glucose in the intestine is transported through two mechanisms, SGLT1 facilitates active transport of glucose from the small intestinal lumen to the epithelial cells, particularly at low glucose concentrations (Gorboulev et al., 2012). GLUT2, on the other hand, facilitates the facilitated diffusion of glucose from epithelial cells to the interstitial space and eventually across the basement membrane into the bloodstream (Dai et al., 2016). In our study, TPS treatment significantly reduced the mRNA and protein expressions of SGLT1 compared to the MC group (Fig. 6). At a concentration of $600\,\mu g\,mL^{-1}$, TPS caused a significant 23.67% reduction in SGLT1 mRNA expression (Fig. 6A). TPS at $400\,\mu g\,mL^{-1}$ and $600\,\mu g\,mL^{-1}$ also significantly decreased GLUT2 mRNA expression (Fig. 6B). Similarly, TPS significantly reduced the protein expression levels of SGLT1 and GLUT2 (Fig. 6C). In diabetic models, SGLT1 and GLUT2 expression levels were up-regulated, and the inhibition of glucose transport mediated by SGLT1 was dependent on Na^+ (Williamson 2013; Liu et al., 2021). Additionally, the combination of green tea TPS and flavonol significantly inhibited the
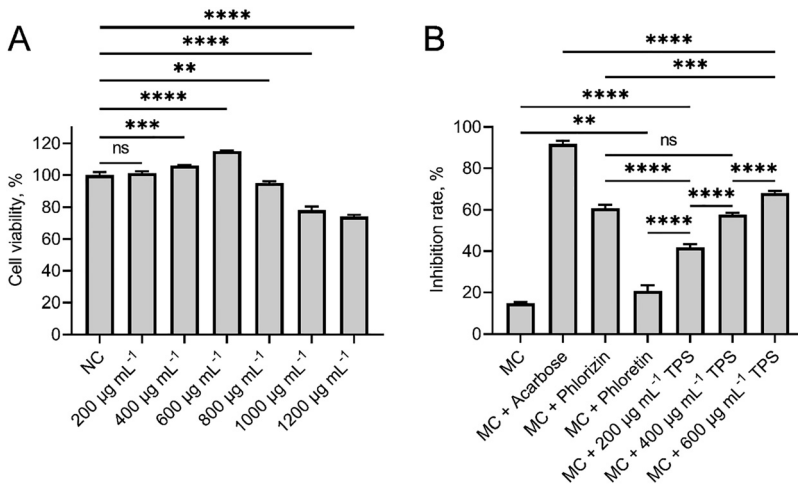

Fig. 5. Caco-2 cell viability and glucose transport. *: $P < 0.05$; **: $P < 0.01$; ***: $P < 0.001$; ****: $P < 0.0001$; ns: not significant
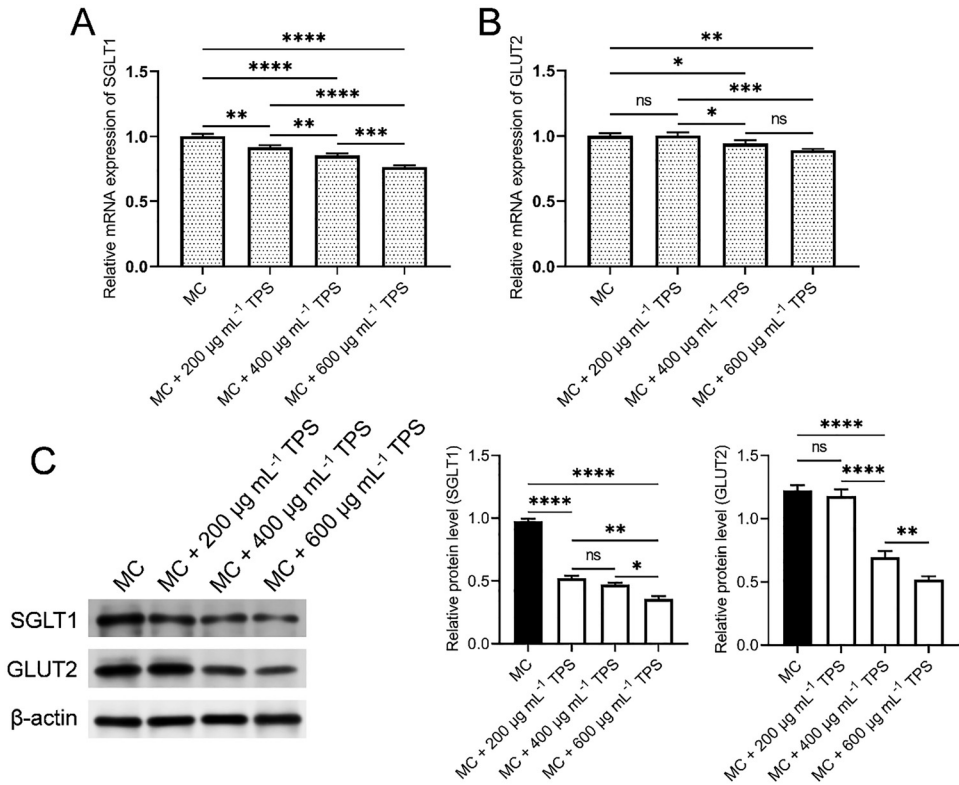
Fig. 6. SGLT1 and GLUT2 mRNA (A, B) and protein (C) expressions. *: $P < 0.05$; **: $P < 0.01$;
***: $P < 0.001$; ****: $P < 0.0001$; ns: not significant

mRNA expression of SGLT1 and GLUT2, leading to delayed blood glucose absorption (Lee et al., 2020; Oh et al., 2021). Previous studies have shown that green tea extracts, including TPS, can inhibit SGLT1 activity and reduce glucose transport, with SGLT1 being more sensitive than GLUT2 (Snoussi et al., 2014; Liu et al., 2021). Combining the findings of this study and previous studies, it can be inferred that TPS primarily inhibits glucose uptake by targeting SGLT1, with a lesser effect on GLUT2.

4. CONCLUSIONS

The yield of LBT-TPS could be significantly improved through optimisation methods, resulting in a purified polysaccharide with higher content. The purified TPS was an acidic polysaccharide bound to trace proteins and primarily consisted of →4)-α-D-Galp-(1→. Moreover, it could inhibit the expression of SGLT1 and GLUT2, leading to reduced glucose transport in Caco-2 cells and exerting a hypoglycaemic effect.

ACKNOWLEDGMENTS

SUPPLEMENTARY MATERIALS

Supplementary data to this article can be found online at https://doi.org/10.1556/066.2023.00115.

REFERENCES

Dai, L., Hu, W.W., Xia, L., Xia, M., and Yang, Q. (2016).Transmissible gastroenteritis virus infection enhances SGLT1 and GLUT2 expression to increase glucose uptake. *Plos One*, 11(11): e0165585.

Gorboulev, V., Schürmann, A., Vallon, V., Kipp, H., Jaschke, A., Klessen, D., Friedrich, A., Scherneck, S., Rieg, T., Cunard, R., Veyhl-Wichmann, M., Srinivasan, A., Balen, D., Breljak, D., Rexhepaj, R., Parker, H.E., Gribble, F.M., Reimann, F., Lang, F., Wiese, S., Sabolic, I., Sendtner, M., and Koepsell, H. (2012). Na(+)-D-glucose cotransporter SGLT1 is pivotal for intestinal glucose absorption and glucose-dependent incretin secretion. *Diabetes*, 61(1): 187–196.

Jones, R.B., Alderete, T.L., Kim, J.S., Millstein, J., Gilliland, F.D., and Goran, M.I. (2019). High intake of dietary fructose in overweight/obese teenagers associated with depletion of *Eubacterium* and *Streptococcus* in gut microbiome. *Gut Microbes*, 10(6): 712–719.

Kellett, G.L. and Brot-Laroche, E. (2005). Apical GLUT2: a major pathway of intestinal sugar absorption. *Diabetes*, 54(10): 3056–3062.

Lee, Y.E., Yoo, S.H., Chung, J.O., Park, M.Y., Hong, Y.D., Park, S.H., Park, T.S., and Shim, S.M. (2020). Hypoglycemic effect of soluble polysaccharide and catechins from green tea on inhibiting intestinal transport of glucose. *Journal of the Science of Food and Agriculture*, 100(10): 3979–3986.

Li, J., Wang, D., Xing, X., Cheng, T.-J.R., Liang, P.-H., Bulone, V., Park, J.H., and Hsieh, Y.S.Y. (2019). Structural analysis and biological activity of cell wall polysaccharides extracted from *Panax ginseng* marc. *International Journal of Biological Macromolecules*, 135: 29–37.

Liu, S., Ai, Z., Meng, Y., Chen, Y., and Ni, D. (2021). Comparative studies on the physicochemical profile and potential hypoglycemic activity of different tea extracts: effect on sucrase-isomaltase activity and glucose transport in Caco-2 cells. *Food Research International*, 148: 110604.

Oh, J.H., Lee, C.Y., Kim, J.E., Kim, W.H., Seo, J.W., Lim, T.G., Lee, S.Y., Chung, J.O., Hong, Y.D., Kim, W.G., Yoo, S.J., Shin, K.S., and Shim, S.M. (2021). Effect of characterized green tea extraction methods and formulations on enzymatic starch hydrolysis and intestinal glucose transport. *Journal of Agricural and Food Chemistry*, 69(50): 15208–15217.

Qin, H., Huang, L., Teng, J., Wei, B., Xia, N., and Ye, Y. (2021). Purification, characterization, and bioactivity of Liupao tea polysaccharides before and after fermentation. *Food Chemistry*, 353: 129419.

Qiu, S., Huang, L., Xia, N., Teng, J., Wei, B., Lin, X., and Khan, M.R. (2022). Two polysaccharides from Liupao tea exert beneficial effects in simulated digestion and fermentation model in vitro. *Foods*, 11(19): 2958.

Shen, S., Xu, Z., Feng, S., Wang, H., Liu, J., Zhou, L., Yuan, M., Huang, Y., and Ding, C. (2018). Structural elucidation and antiaging activity of polysaccharide from *Paris polyphylla* leaves. *International Journal of Biological Macromolecules*, 107(Pt B): 1613–1619.

Snoussi, C., Ducroc, R., Hamdaoui, M. H., Dhaouadi, K., Abaidi, H., Cluzeaud, F., Nazaret, C., Le Gall, M., and Bado, A. (2014). Green tea decoction improves glucose tolerance and reduces weight gain of rats fed normal and high-fat diet. *Journal of Nutritional Biochemistry*, 25(5): 557–564.

Wang, Q., Yang, X., Zhu, C., Liu, G., Sun, Y., and Qian, L. (2022). Advances in the utilization of tea polysaccharides: preparation, physicochemical properties, and health benefits. *Polymers*, 14(14): 2775.

Williamson, G. (2013). Possible effects of dietary polyphenols on sugar absorption and digestion. *Molecular Nutrition & Food Research*, 57(1): 48–57.

Wu, Y., Sun, H., Yi, R., Tan, F., and Zhao, X. (2021). Anti-obesity effect of Liupao tea extract by modulating lipid metabolism and oxidative stress in high-fat-diet-induced obese mice. *Journal of Food Science*, 86(1): 215–227.

Zhu, J., Chen, X., Li, F., Wei, K., Chen, J., Wei, X., and Wang, Y. (2022). Preparation, physicochemical and hypoglycemic properties of natural selenium-enriched coarse tea glycoproteins. *Plant Foods for Human Nutrition*, 77(2): 258–264.

Zhu, J., Chen, Z., Chen, L., Yu, C., Wang, H., Wei, X., and Wang, Y. (2019). Comparison and structural characterization of polysaccharides from natural and artificial Se-enriched green tea. *International Journal of Biological Macromolecules*, 130: 388–398.

Zhu, J., Chen, Z., Zhou, H., Yu, C., Han, Z., Shao, S., Hu, X., Wei, X., and Wang, Y. (2020a). Effects of extraction methods on physicochemical properties and hypoglycemic activities of polysaccharides from coarse green tea. *Glycoconjugate Journal*, 37(2): 241–250.

Zhu, J., Du, M., Wu, M., Yue, P., Yang, X., Wei, X., and Wang, Y. (2020b). Preparation, physicochemical characterization and identification of two novel mixed ACE-inhibiting peptides from two distinct tea alkali-soluble protein. *European Food Research and Technology*, 246(7): 1483–1494.

Zhu, J., Wu, M., Zhou, H., Cheng, L., Wei, X., and Wang, Y. (2021a). Liubao brick tea activates the PI3K-Akt signaling pathway to lower blood glucose, metabolic disorders and insulin resistance via altering the intestinal flora. *Food Research International*, 148: 110594.

Zhu, J., Yu, C., Han, Z., Chen, Z., Wei, X., and Wang, Y. (2020c). Comparative analysis of existence form for selenium and structural characteristics in artificial selenium-enriched and synthetic selenized green tea polysaccharides. *International Journal of Biological Macromolecules*, 154: 1408–1418.

Zhu, J., Yu, C., Zhou, H., Wei, X., and Wang, Y. (2021b). Comparative evaluation for phytochemical composition and regulation of blood glucose, hepatic oxidative stress and insulin resistance in mice and HepG2 models of four typical Chinese dark teas. *Journal of the Science of Food and Agriculture*, 101(15): 6563–6577.

Zhu, J., Zhou, H., Zhang, J., Li, F., Wei, K., Wei, X., and Wang, Y. (2021c). Valorization of polysaccharides obtained from dark tea: preparation, physicochemical, antioxidant, and hypoglycemic properties. *Foods*, 10(10): 2276.